J. Agr. Sci. Tech. (2011) Vol. 13: 251-262

Unsteady Free Surface Flow in Corrugated Drainage Pipes: Finite Volume Solution and Experimental Verification

M. M. Heidari[1], S. Kouchakzadeh[1]*, and E. Bayat[1]

ABSTRACT

A subsurface drainage network mainly carries unsteady flow and data are not usually available for model parameters calibration in such networks. In the present research, the finite volume method using the time splitting scheme was employed to develop a computer code for solving the one dimensional unsteady flow equations. Using corrugated sub-drainage pipes, an experimental prototype setup was constructed to examine the numerical model response in predicting the observed unsteady data in such circumstances. The experimental setup components and the model parameters were calibrated in place based on steady state flow condition. The results revealed satisfactory performance by the abovementioned method and the scheme employed and justified its validity for field application.

Keywords: Corrugated drainage pipe, Finite volume method, Time splitting scheme, Unsteady flow.

INTRODUCTION

Various numerical methods for solving partial differential equations have been developed that could generally be classified as characteristic method, finite difference, finite element, boundary element, spectral and finite volume methods (Chaudhry, 2008). Stoker (1957) proposed an explicit scheme based on the characteristic method for solving the Saint de Venant Equations. Preissmann (1960) developed the four point finite difference scheme for solving the one dimensional unsteady flow equations. Numerous hydrodynamic models employed the Preissman's scheme so far. Abbott (1966 and 1979) proposed the six point scheme which has been used in Mike 11 hydrodynamic model. Moretti (1979) developed the Lambda scheme which was evaluated by Chaudhry and Fennema (1979). Patankar (1980) presented the finite volume method. Namin et al. (2007a) employed the finite volume method and the time splitting technique for solving the governing equation and compared its results with that of Mike 11 and concluded that the scheme provided rather reasonable results.

Published data concerning experimental unsteady flow research are very limited compared to that of numerical investigations. The reason could be attributed to the cost, time, and the inherent difficulties of the experimental investigations, especially in the complexity of the unsteady flow phenomenon. Martin-Vide et al. (1993) reported data of moving wave fronts in a rectangular flume. They generated steep moving wave fronts in steady discharges of 15 and 45 l/s by changing the downstream boundary condition of the flume. Zahang and Summer (1999) compared the field data of influence of sudden closure of turbine gates on the upstream flow condition of the Drau river with that of Floris numerical model and

[1] Irrigation and Reclamation Engineering Department, University of Tehran, P. O. Box 31587-4111, Karaj, 31587-77871 Islamic Republic of Iran.
* Corresponding author, e-mail: skzadeh@ut.ac.ir

[DOR: 20.1001.1.16807073.2011.13.2.5.0]

reported good agreement. Tseng et al. (2001) verified their proposed chock capturing schemes by using dam break experimental data. Parvaresh-Rizi et al. (2005) experimentally investigated the unsteady transcritical flow in tilting rectangular flume and proposed empirical relationships for estimating the conjugate depths of a moving hydraulic jump. Soares (2007) experimentally studied the influence of triangular shape baffles installed at a dam toe on the dam break flood wave behavior. Monem et al. (2006) applied a hydrodynamic model to simulate the unsteady flow along an irrigation channel caused by temporal variations in flow deliveries of different offtakes and evaluated the impact of the unsteady flow on the hydraulic performance appraisal indices of the network.

Advanced codes and modeling tools were developed during the last five decades as the outcome of extensive numerical research. However, "reliable" experimental and field data for evaluating the developed codes and modeling tools are very limited and could not easily be accessed. The need for data concerning unsteady state flow was highlighted in the published materials during the last few years. The Association of Hydraulic Engineering and Research published a supplementary issue in 2007 of the Journal of Hydraulic Research entitled "Dam break flow experiments and real-case data". Greco (2008) considered the development of numerical models without the presence of experimental data for evaluating the model prediction as a futile exercise and believed that parameter sensitivity could not be considered as substitute for comprehensive model verification by using experimental and field data. Greco (2008) highlighted the need for actively encouraging experimental research and making the data available to numerical researchers. Cunge (2008) also believes in the absolute necessity of several types of data, specially when dealing with mechanistic models. The available field data allowing for model calibration are, in general, polluted by different influences and, therefore, there is a need for reliable data (Cunge, 2008).

Corrugated pipes are the main component in constructing a drainage network around the world. Subsurface drainage networks operate mainly under unsteady flow condition, but, their underground installation usually does not allow flow visualization along the network pipes and makes unsteady model calibration impractical. Indeed, the objectives of the current study are to experimentally determine the calibration parameters (major and minor head losses) to a certain degree of accuracy using steady state flow condition data that are supposedly available to the designer. These factors would then be plugged into the unsteady state model to examine its prediction capability based on the employed parameters. Also, the performance of the finite volume method using the time splitting scheme, which has not been experimentally verified yet, will be reported.

MATERIALS AND METHODS

Experimental Setup

The experimental setup was constructed using two reaches of a corrugated drainage pipe each 4.3 meters long connected to a cylindrical "Flow-through" type manhole in between. The manhole diameter was 0.6m. The experimental setup and details of the pipe characteristics are presented in Figure 1.Twenty seven piezometer taps were connected along the pipe invert and around the manhole wall. Water was circulated in the system by using two centrifugal pumps one of which was equipped with Micromaster Drive for providing variable rotational speed by changing the frequency and the voltage of the electrical current. The suction pipe of the upstream pump was connected to the main storage reservoir and its discharge pipe delivered the water to an entrance tank located at the upstream side of the corrugated pipe. The entrance take was

[DOR: 20.1001.1.16807073.2011.13.2.5.0]

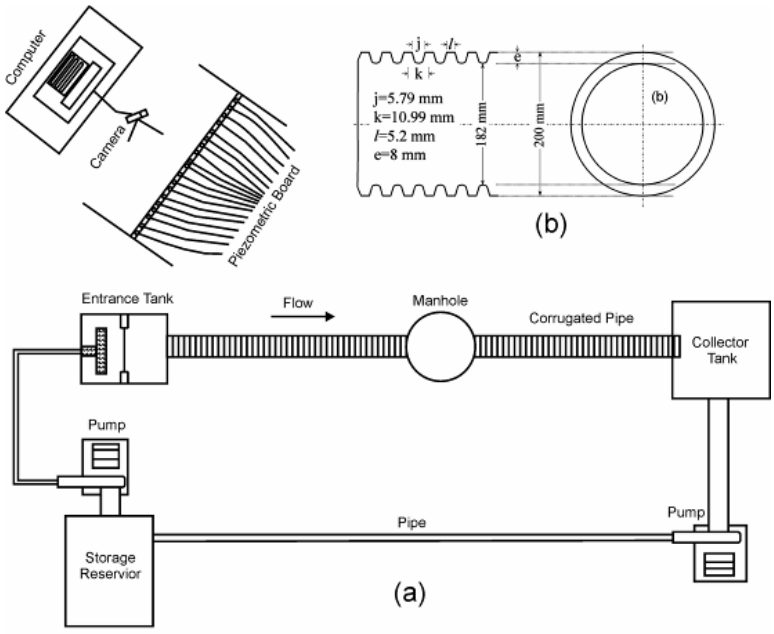

Figure 1. (a) Schematic of the experimental setup plan (b) details of the corrugated pipe.

equipped with a turbulence reduction system and a 135° V-notch weir as a measuring device. Measured water entered the upstream segment of the corrugated pipe and, after passing the manhole, it moved through the downstream segment to reach the brink of the pipe. Underneath the downstream end of the corrugated pipe, a tank was installed to collect the water from the pipe brink. Water accumulated at the collector tank was then pumped to the storage tank by using a constant rotational speed pump to complete the water circulation cycle. The variable rotational speed pump provided the ability of generating variety of hydrograph shapes.

The data acquisition system consisted of a piezometric board holding all the system piezometers, a high definition camcorder, and software for framing and digitizing the records. Compiled data were meant for assessing the computer code performance. Therefore, the data should be free of pollution and directly related to each parameter referred to. Such data is generally neither easily accessible nor readily experimentally collectable. Therefore, prior to starting the main tests, extensive work was done to determine the empirical invariant coefficients such as flow resistance and head loss coefficients and to calibrate different components of the setup including V-notch weir and brink depth discharge relationship at the downstream end of the pipe. The V-notch weir was calibrated in place based on the volumetric method. The result is depicted in Figure 2.

Flow resistance, however, is usually subject to serious uncertainty and should be given a special attention. Therefore, regardless of the wide range of Manning's n coefficient proposed in the literature, the inverse method was used to determine the

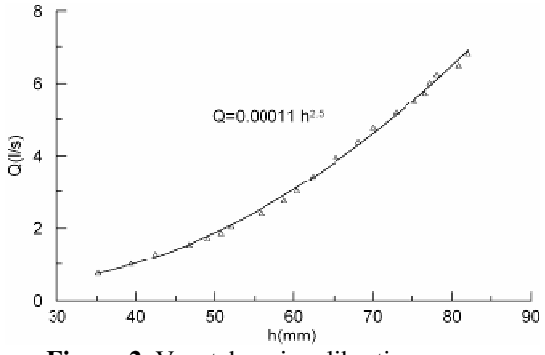

Figure 2. V-notch weir calibration curve.

[DOR: 20.1001.1.16807073.2011.13.2.5.0]

flow resistance coefficient. That is, a very wide discharge range and longitudinal slopes were tested to produce gradually varied flows along the conduit. The water surface elevation from the brink of the pipe to its upstream end was recorded for each discharge. Then, the gradually-varied-flow governing equation was solved repeatedly for different n values to determine the most suitable resistance coefficient that provided the best agreement between the observed and the computed values. The result is shown in Figure 3, which reveals that an average value of n=0.02 could be used practically.

The local head loss associated with the manhole was also determined by balancing the energy grade line at the manhole entrance and exit based on the compiled experimental data. Figure 4 presents the variation of the head loss coefficient against the discharge. The figure Indicates that applying an average value of K=1 for the head loss coefficient would collapse the observed and computed data around the line of perfect agreement with the maximum errors of ±10%.

The boundary condition at the downstream end of the conduit is also required in this research. The flow left the downstream end of the pipe in the form of free overfall, therefore, the brink depth-discharge ratio should be determined experimentally. The recorded depth-discharge relationship is presented in Figure 5; it was employed as the downstream boundary condition in the numerical solution.

Basically, the unsteady water surface elevations along the pipe and other setup component were recorded via the variations observed on the piezometers installed on the piezometric board. The concurrence of the water surface elevation within the setup components and that of the respected piezometers installed on the piezometric board should be examined and justified. In this regard, the impacts of the piezometer hose lengths and temporal drawdown rates on the mentioned water surface elevations were thoroughly tested. The results indicated that within the piezometer hose lengths and temporal drawdown and rising rates experienced in this research the water surface elevations recorded on the piezometric board practically represent the water surface elevation of the corresponding points of the setup.

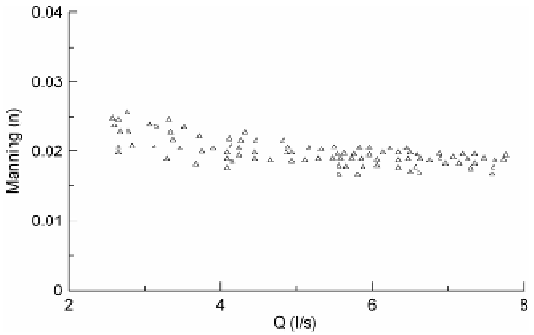

Figure 3. Variation of Manning's coefficient in corrugated pipes.

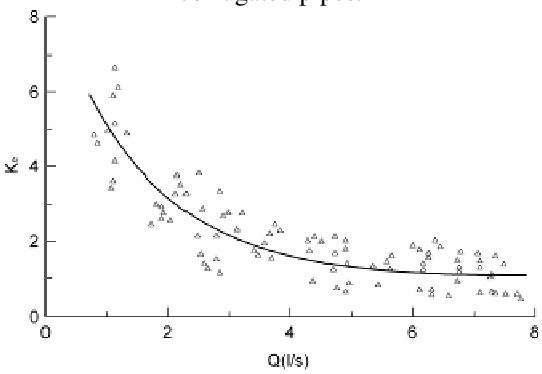

Figure 4. Variation of head loss coefficient associated with the manhole (Azimi et al., 2008).

Arrangement of Unsteady Flow Experiments

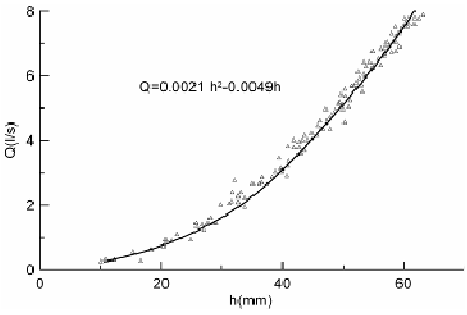

Figure 5. Brink depth-discharge relationship at the down stream end of the conduit.

[DOR: 20.1001.1.16807073.2011.13.2.5.0]

A hydrograph could be generated simply by defining three parameters on the Micromaster drive i.e. the maximum output frequency, the ramp up, and the ramp down times. For instance, considering given values of the mentioned parameters, the selected frequency determines the maximum rotational speed and, consequently, the peak discharge of the hydrograph. The ramp up and the ramp down times set the rising and falling stages periods from an initial discharge condition to the peak flow and back to the initial stage, respectively. As a result, a variety of hydrograph shapes could be generated by applying different parameter values to the Micromaster drive. Data recording was synchronized with the start up time of the pump, but, it was continued beyond its shut down until the water was depleted form the pipe. Recorded water surface elevation movements were then framed and digitized to produce the water surface elevations along the corrugated pipe and other setup components.

Governing Equations of the Unsteady Flow

The continuity and momentum equations employed in this research were as follows (Cunge et al., 1980):

$$\frac{\partial y}{\partial t}+\frac{1}{T}\frac{\partial Q}{\partial x}=0 \qquad (1$$

$$\frac{\partial Q}{\partial t}+\frac{\partial}{\partial x}(uQ)+gA\frac{\partial y}{\partial x}=-gA(S_f+S_e) \qquad (2$$

where t is time, x is distance, g is acceleration due to gravity, Q is discharge, A is cross sectional area of the flow, y is water surface elevation with respect to a given datum, T is top width of the water section, u is flow velocity, S_f is friction slope, and S_e is minor head loss.

Time Splitting Scheme

To apply the time splitting scheme for solving the governing equations, the convectional acceleration term of Equation (2) i.e. the second term on the left hand side should be separated and solved explicitly for all the grids of the entire computational domain. In the next stage, energy losses terms (friction and minor head loss) should be separated from the same equation and solved for the entire domain. Finally, the terms left over from the momentum equation should simultaneously be solved with the continuity equation. In this method, the governing equations are solved on a staggered grid according to Figure 6.

Accordingly, the flow depth values are determined in the middle of the control volumes while the flow velocity and

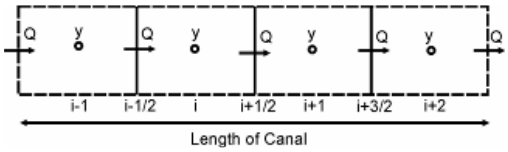

Figure 6. Staggered grid used for the time splitting scheme.

discharge values were computed on the control volume boundaries (Namin et al., 2007a).

Discretization of the Convectional Acceleration Term

To discretize the convectional acceleration term in the time splitting technique different schemes might be used. In this paper, Fromm scheme will be used according to the following equation (Namin et al., 2007b):

$$Q_i^* = Q_i^j - \frac{1}{2}(Q_{i-1}^j - Q_{i+1}^j)\varepsilon + \frac{1}{2}(Q_{i-1}^j - 2Q_i^j + Q_{i+1}^j)\varepsilon^2 \quad (3$$

$$\varepsilon = \frac{u\Delta t}{\Delta x}$$

Where j is current time step, i is the current spatial step, ε is Courant number, Δt is time step, Δx is distance step, and Q_i^* is the new value of the discharge. Other parameters were previously defined. It should be mentioned that Fromm scheme presents the second order accuracy. A scheme of higher order of accuracy might be used in this stage, however, according to the schemes used to discretize other terms of the governing equation, the employed accuracy

[DOR: 20.1001.1.16807073.2011.13.2.5.0]

could be regarded appropriate (Namin et al., 2007b).

Discretization of Friction Terms

After solving the acceleration term, the friction terms according to Equation (4) were separated form the momentum equation and discretized in the form presented by Equation (5).

$$\frac{\partial Q}{\partial t} = -gA(S_f + S_e) \quad (4$$

$$Q_i^{**} = Q_i^* - gA_i\Delta t(S_{fi}^* + S_{ei}^*) \quad (5$$

Where Q_i^{**} is the new discharge trail value and other parameters were previously defined. Manning's equation was used to evaluate the friction slope and the manhole was considered as a computational cell in which the energy loss gradient could be determined according to Equation (6)

$$S_e^* = K_e \frac{u_e^{*2}}{2gD} \quad (6$$

Where $S_e^*$is local energy loss gradient, $u_e^*$is pipe flow velocity at the manhole downstream connection, D is manhole diameter, and K_e is head loss coefficient.

Discretization of the Continuity Equation and the Gravitational Term of the Momentum Equation

The continuity equation and the gravitational term of the momentum equation should be discretized according to Equations (7) and (8) and solved succeeding the solution of the previously mentioned terms of the momentum equation. Incorporating the weighting factor α in the formulation provides access to either explicit or implicit solution forms.

$$\frac{y_i^{j+1} - y_i^j}{\Delta t} + \frac{1}{\Delta x T_i^j}\left(Q_{i+1/2}^{j+1} - Q_{i-1/2}^{j+1}\right) = 0 \quad (8$$

Combining Equations (7) and (8) and simplifying the results yields Equation (9) for the interior node of the solution domain.

$$B_i^1 y_{i-1}^{j+1} + B_i^2 y_i^{j+1} + B_i^3 y_{i+1}^{j+1} = B_i^0 \quad (9$$

Where $B_{i's}$ are coefficients computed according to Equations (10) to (13) in each time step.

$$B_i^1 = -(1-\alpha) g \frac{\Delta t A_{i-1/2}^j}{\Delta x^2 T_i^j} \quad (10$$

$$B_i^2 = \frac{1}{\Delta t} + (1-\alpha) g \frac{\Delta t A_{i-1/2}^j}{\Delta x^2 T_i^j} + (1-\alpha) g \frac{\Delta t A_{i+1/2}^j}{\Delta x^2 T_i^j} \quad (11$$

$$B_i^3 = -(1-\alpha) g \frac{\Delta t A_{i+1/2}^j}{\Delta x^2 T_i^j} \quad (12$$

$$B_i^0 = \frac{y_i^j}{\Delta t} - \frac{1}{\Delta x T_i^j}(Q_{i+1/2}^{**} - Q_{i-1/2}^{**}) - \alpha g \frac{\Delta t}{\Delta x^2} \frac{A_{i-1/2}^j}{T_i^j}(y_i^j - y_{i-1}^j) + \alpha g \frac{\Delta t}{\Delta x^2} \frac{A_{i+1/2}^j}{T_i^j}(y_{i+1}^j - y_i^j) \quad (13$$

Incorporating the boundary conditions in the solution, a tri-diagonal system of equations was obtained that was solved by Thomas algorithm method to provide the solution for y^{j+1} for all computational nodes (Hoffmann and Chiang, 2000).

Initial and Boundary Conditions

The water surface elevation and the discharge for the entire computational nodes were determined and used as the initial condition at the first time step. Also, the water surface elevations and the brink depth-discharge relationship were used as the upstream and downstream boundary conditions, respectively.

$$\frac{Q_{i+1/2}^{j+1} - Q_{i+1/2}^{**}}{\Delta t} + gA_{i+\frac{1}{2}}^j \frac{1}{\Delta x}\left[\alpha\left(y_{i+1}^j - y_i^j\right) + (1-\alpha)\left(y_{i+1}^{j+1} - y_i^{j+1}\right)\right] = 0 \quad (7)$$

[DOR: 20.1001.1.16807073.2011.13.2.5.0]

Numerical Scheme Assessment Criteria

To evaluate the performance of the numerical scheme, the observed and the computed values were compared by using the following criteria (Jabro et al., 1998):

$$RMSE = \left[\frac{1}{k}\sum_{i=1}^{k}\left(m_i - s_i\right)^2\right]^{0.5} \quad (14$$

$$EF = \frac{\sum_{i=1}^{n}\left(m_i - M\right)^2 - \sum_{i=1}^{n}\left(m_i - s_i\right)^2}{\sum_{i=1}^{n}\left(m_i - M\right)^2} \quad (15)$$

$$CRM = \frac{\sum_{i=1}^{n} m_i - \sum_{i=1}^{n} s_i}{\sum_{i=1}^{n} m_i} \quad (16$$

$$MAPE = \frac{100}{k}\sum_{i=1}^{k}\left|\frac{m_i - s_i}{m_i}\right| \quad (17$$

Where k is number of observed or measured point and s_i, m_i, and M stand for the simulated, measured (observed), and average of flow depth, respectively. The root mean square error (*RMSE*) provides a percentage for the total difference between simulated and measured values proportioned against the mean observed values. The lower limit for *RMSE* is zero which indicates the most accurate simulation. The modeling efficiency (*EF*) is a measure for assessing the accuracy of simulations. For perfect concurrence, *EF* becomes unity. The coefficient of residual mass (*CRM*) is an indication of the consistent errors in the distribution of all simulated values across all measurements with no consideration of the order of the measurements. A *CRM* value of zero denotes no bias in the distribution of the simulated values with respect to the measured values. *MAPE* is the mean absolute percent error of estimation; the closer is *MAPE* to zero, the better are the results.

RESULTS AND DISCUSSION

The previously presented relationships were used to develop a computer code in Compaq Visual Fortran. Prior to running the code for unsteady flow, its performance for steady state initial and boundary conditions was evaluated, which provided the anticipated results and justified the code application for the next step. Accordingly, a number of flood hydrographs were run through the experimental setup and the data were recorded and tabulated for evaluating the code performance. Then, the outputs of the computer code that were obtained for the same initial and boundary conditions data of the experimental runs were compared with that of the observed values.

The computed and observed stage hydrograph at the manhole and a section 3700mm downstream of the manhole are presented in Figure 7. Equations (14) to (17) were applied to the computed stage hydrograph at the manhole and a section 3700mm downstream of the manhole and the corresponding observed values. The results of the evaluation parameters determined for comparing stage hydrographs are presented in Table 1.

Generally, they indicate good agreement between the computed and the observed

Table 1. Assessment criteria for the stage hydrograph of given tests at specified stations.

Test	Assessment Criteria							
	RMSE		EF		CRM		MAPE	
	S1*	S2	S1	S2	S1	S2	S1	S2
A	4.03	5.56	0.97	0.93	0.009	0.052	4.93	6.94
B	3.28	5.39	0.94	0.97	0.041	0.034	4.27	4.04
C	4.66	5.13	0.87	0.8	0.073	0.117	6.88	12.55
D	5.86	3.57	0.94	0.97	0.05	0.052	5.85	4.77
E	5.84	4.07	0.88	0.91	0.016	0.001	4.4	4.77
F	4.35	3.75	0.96	0.96	0.069	0.083	6.79	7.61

S: station

[DOR: 20.1001.1.16807073.2011.13.2.5.0]

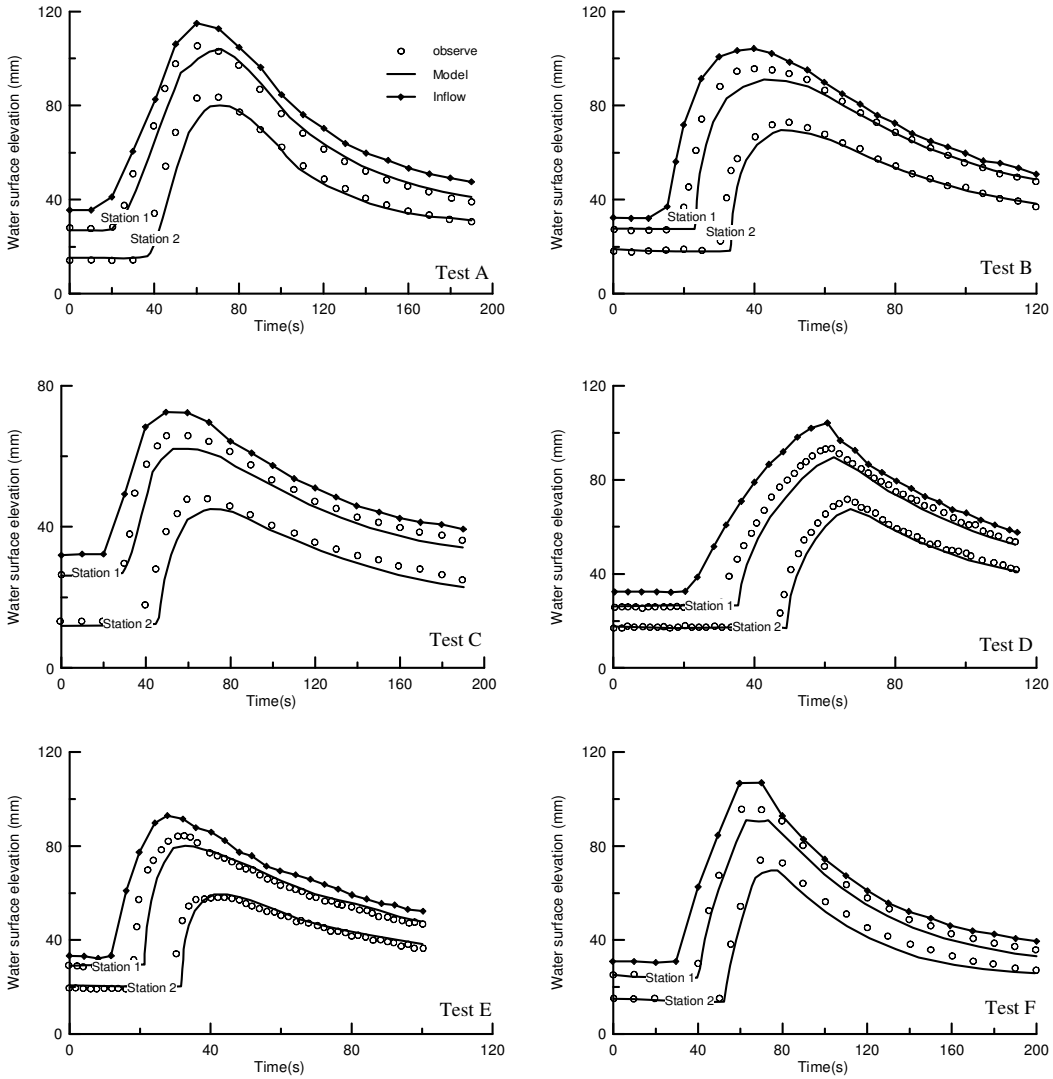

Figure 7. Comparison between the observed and the computed stage hydrographs at two stations.

values. Close attention to the results shows that the errors associated with the rising stage are higher than that of the falling stage. This could be attributed to the higher temporal variation rate of the rising stage compared to the falling one. Evidently, applying the boundary conditions based on steady state conditions for high temporal variation rate would result in higher error in the computation results.

The computed water surface profile and the corresponding observed ones are presented in Figure 8 and the average of the computed assessment parameters are presented in Table 2. According to the assessment parameters given in Table 2, the model was able to predict the unsteady water surface profiles with reasonable accuracy without prior calibration of the model parameters. It should be emphasized that the stage-discharge relationship of the brink and the major and the minor head losses were determined using steady state flow condition. This result could be of great practical interest for circumstances such as sub-drainage networks where calibration data is not easily available.

Additionally, to investigate the impact of the major and the minor head loss coefficient variations on the results, a sensitivity analysis was carried out. As mentioned earlier, the coefficients were

[DOR: 20.1001.1.16807073.2011.13.2.5.0]

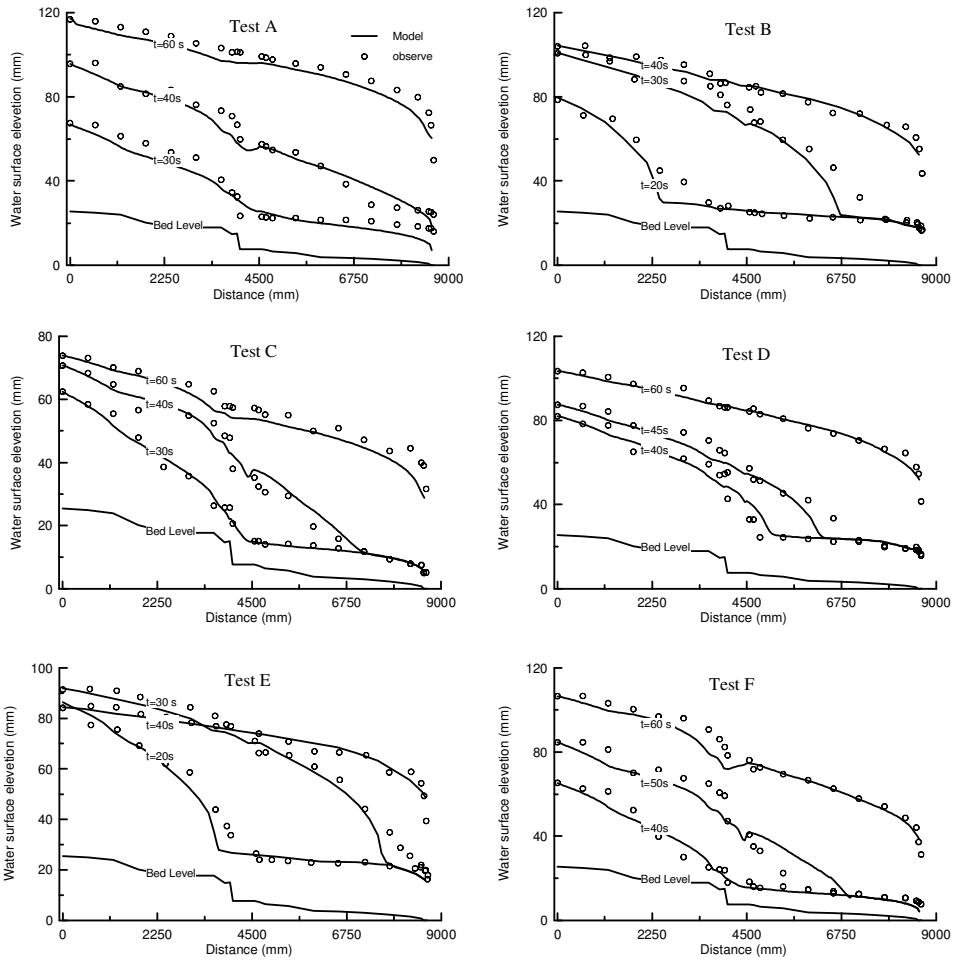

Figure 8. Comparison between the computed and the observed water surface profile.

experimentally determined using wide test conditions (Figures 3 and 4). The sensitivity analysis was performed according to the variation range of n and K_e observed in Figures 3 and 4 and the results of RMSE for test D are indicted in Figure 9 as a sample plot. It should be mentioned that other tests demonstrated similar results. Figure 9 generally points out that n-values between 0.017 and 0.02 show good performance regardless of the selected K_e-value. However, the least RMSE was obtained using the proposed coefficients, i.e. K_e=1 and n=0.02.

It is worth mentioning that the stage discharge relationships and other empirical coefficients determined by using steady state flow tests might demonstrate different values in unsteady flow condition since the energy gradient is continually changing in this condition and, therefore, introduces higher error value in the computational

Table 2. Assessment criteria for the water surface profile of some tests.

Criteria	Test					
	A	*B*	*C*	*D*	*E*	*F*
RMSE	4.86	4.21	2.81	3.69	3.59	4.74
EF	0.92	0.96	0.946	0.965	0.96	0.95
CRM	0.053	0.033	0.017	0.01	0.03	0.035
MAPE	9.97	6.02	7.22	5.74	5.58	11.3

[DOR: 20.1001.1.16807073.2011.13.2.5.0]

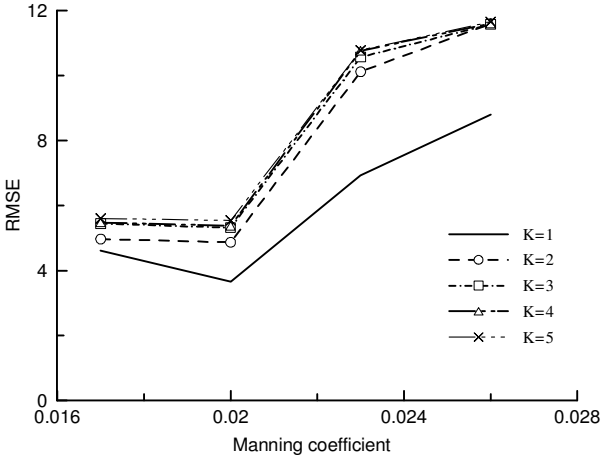

Figure 9. Variation of RMSE against different n and K_e values for test D.

nodes close to the boundaries. However, it seems that no feasible method has been proposed yet for evaluating such coefficients and relationships in unsteady state condition because of the excessive inherent complexity of the phenomenon.

CONCLUSION

The research presented a computational code developed based on the finite volume method, the time splitting scheme, and an experimental setup to evaluate the code performance using predefined calibration parameters. Different components of the experimental setup were calibrated in place and the major and the minor head losses were determined based on the compiled steady state data to ensure reliable comparison results between the observed and the computed values. The results indicated that, generally, the mathematical code performed well enough and the proposed coefficient that was determined based on prototype scale experimental setup could be applied for field situations.

ACKNOWLEDGEMENT

The research was supported by the Iranian National Science Foundation. The authors gratefully acknowledge the INSF financial support and the laboratory facilities provided by the Center of Excellence for Evaluation and Rehabilitation of Irrigation and Drainage networks.

Nomenclature

The following symbols are used in this paper:

A=cross sectional area of the flow (m^2)
B_i^0, B_i^1, B_i^2, B_i^3=coefficients in continuity equation and the gravitational term of the momentum equation
CRM=coefficient of residual mass
D=manhole diameter (m)
EF= modeling efficiency
g=acceleration due to gravity (m/s^2)
i=current spatial step
j=current time step
k=number of observed or measured points of flow depth
K_e=head loss coefficient
M=average of flow depth (m)
$MAPE$= mean absolute percent error
m=measured flow depth (m)
n= Manning's coefficient of roughness
Q=discharge (m^3/s)
$RMSE$=root mean square error
S_e=local energy loss gradient (m/m)
S_f= friction slope (m/m)
s_i=simulated of flow depth (m)

[DOR: 20.1001.1.16807073.2011.13.2.5.0]

t=time (s)
T=top width of the water section (m)
u= flow velocity (m/s)
u_e^* =pipe flow velocity at the manhole downstream connection (m/s)
x=distance (m)
y=water surface elevation with respect to a given datum (m)
Δt=time step (s)
Δx=distance step (m)
α=weighting coefficient for explicit or implicit solution forms
ε=Courant number

REFERENCE

1. Abbott, M. B. 1966. An Introduction to the Method of Characteristics. Thames and Hudson, London, American Elsevier, New York.
2. Abbott, M. B. 1979. Computational Hydraulics; Elements of the Theory of Free Surface Flows. Pitman Publishing Ltd., London.
3. Azimi, R., Kouchakzadeh, S. and Bayat, E. 2008. Determination of Minor Head Loss at Manhole and Junction in Subsurface Drainage Networks. 7th Iranian Hydraulic Conference, Power and Water University Of Technology , Tehran, Iran.
4. Chaudhry, M. H. 2008. Open Channel Flow. Springer, New York, USA.
5. Cunge, J. A., Holly, F.M., Vervey, Jr. and A. 1980. Practical Aspect of Computational River Engineering. Pitman Advanced Publishing Program, London, UK.
6. Cunge, J. A. 2008. Numerical Models, Data and Predictability. *Hyrolink, IAHR*, **3**: 39-40.
7. Fennema, R. J. and Chaudhry, M. H. 1987. Simulation of One Dimensional Dam Break Flows. J. Hydraulic Res., Vol.25(1), 41-51.
8. Greco, M. 2008. Numerical Modeling Research a Xmas Wish. *Hyrolink, IAHR*, **1**: 12-13.
9. Hoffmann, K. A. and Chiang, S. T. 2000. Computational Fluid Dynamics for Engineers. Vol. I, Engineering Education Systems, Wichita State University, Kansas.
10. Jabro, J. D., Toth, J. D. and Fox, R. H. 1998. Evaluation and Comparison of Five Simulation Models for Estimating Water Drainage Fluxes Under Corn. *J. Environmental Quality*, **27**: 1376–1381.
11. Martinvide, J. P., Dolz, J. and Estal, J. D. 1993. Kinematics of the Moving Hydraulic *Jump. J. Hydraulic Res.*, **31(2)**: 171-186.
12. Monem, M. J., Ghodousi, H. and Emadi, A. R. 2006. Quantifying Operation Performance of Irrigation Canals in Response to Demand Variation Using Hydrodynamic Model and Analysis of Unsteady Flow. *J. Agricultural Research (Water, Soil, Plant)*, **6**: 17-29.
13. Moretti, G. 1979. The Lambda Scheme. *J. Computers and Fluids*, **7**:191-205.
14. Namin, M. M., Bohluly, A., Alahdin, S., Ranjbaran, L. and Mohammadzadeh, M. 2007a. Flow Simulation in River Networks by Time-Splitting Method and Comparison with Mike11 Model. 7th International River Engineering Conference , Shahid Chamran University, Ahwaz, Iran.
15. Namin, M. M. and Bohluly, A. 2007b. Numerical Simulation of Free Surface Flow Using Projection Method on Rectangular Structured grid and Triangular Unstructured Grid. 7th International River Engineering Conference, Shahid Chamran University, Ahwaz, Iran.
16. Parvaresh-Rizi, A., Kouchakzadeh, S. and Omid, M. H. 2005. Unsteady Transcritical Flow in Rectangular Channels. 31st International IAHR Congress, Seoul, Korea.
17. Patankar, S. V. 1980. Numerical Heat Transfer and Fluid Flow. Hemisphere Corporation, USA.
18. Preissmann, A. 1960. Propagation des intumescences dans les canaux et rivières. First Congress of the French Association for Computation, AFCAL Grenoble, France, 433-442.
19. Soares, F. S. 2007. Experiments of Dam-Break Wave Over a Triangular Bottom Sill. *J. Hydraulic Res.*, **45**: 19–26.
20. Stoker, J. J. 1957. Water waves, Interscience, New York, 331-341.
21. Tseng, M. H., Hsu, C. A. and Chu, C. R. 2001. Channel Routing in Open Channel Flow with Surges. *J. Hydraulic Eng.*, **127(2)**: 115-122.
22. Zahang, W. and Summer, W. 1999. Computation of Rapidly Varied Unsteady Flows in Open Channels and Comparison with Physical Model and Field Experiment. 28th IAHR Congress, Granz, Austria.

[DOR: 20.1001.1.16807073.2011.13.2.5.0]

جریان غیرماندگار با سطح آزاد در مجرای موج‌دار زهکشی: روش عددی حجم محدود و مقایسه آزمایشگاهی

م. م. حیدری، ص. کوچک‌زاده و ا. بیات

چکیده

یک شبکه زهکش زیر زمینی اساساً جریان غیر ماندگار را منتقل می‌کند و داده‌های مورد نیاز برای تطبیق و مدل قابل تحصیل در چنین شبکه‌هایی در دسترس نیست. در این پژوهش، با استفاده از روش حجم محدود و با کاربرد شمای تنصیف زمان، معادلات جریان غیرماندگار مجاری روباز با ترکیبی از روش‌های صریح و ضمنی حل شده و یک مدل یک بعدی برای شبیه‌سازی جریان در مجاری موج‌دار ارائه شده است. به منظور ارزیابی عملکرد مدل عددی توسعه یافته، یک مدل فیزیکی مقیاس واقعی طراحی و احداث شد. ابتدا به منظور تعیین ضرایب مقاومت کلی و موضعی اجزای مدل فیزیکی آزمایش‌های متعددی به اجرا در آمد تا نتایج مقایسه ستاده مدل عددی با مشاهدات آزمایشگاهی حتی الامکان متأثر از عدم قطعیت‌های نهفته در کالیبراسیون نباشد. سپس هیدروگراف‌های متنوع جریان غیرماندگار آزمون شد و تغییرات نسبت به زمان پارامترهای مورد نظر ثبت گردید. مقایسه نتایج بدست آمده از اجرای مدل عددی برای جریان‌های غیرماندگار نشان می‌دهد که انطباق قابل قبولی بین داده‌های آزمایشگاهی و نتایج عددی وجود دارد که کارآیی روش و ضرایب تعیین شده را برای کاربرد میدانی تبیین می‌کند.

[DOR: 20.1001.1.16807073.2011.13.2.5.0]